04,09

Electronic structure and shallow traps nature in silicon-enriched SiO_xN_y: *ab initio* simulation

© T.V. Perevalov[1], D.R. Islamov[1,2], V.A. Volodin[1,2]

[1] Rzhanov Institute of Semiconductor Physics, Siberian Branch, Russian Academy of Sciences, Novosibirsk, Russia
[2] Novosibirsk State Technical University, Novosibirsk, Russia

E-mail: timson@isp.nsc.ru

Received October 9, 2024
Accepted October 9, 2024
Revised October 11, 2024

Within the *ab initio* simulation, SiO_xN_y model structures in a wide range of compositions were created, whose short-range order corresponds to the random bonding model. SiO_xN_y energy diagrams were constructed: the dependence of the position of the valence band top and conduction band bottom on the composition of x and y relative to the vacuum level. The electronic structure of native defects in SiO_xN_y that are involved in charge transport was studied. It has been found that Si−Si bonds in SiO_xN_y can produce shallow traps with energies in the range of 10−100 meV.

Keywords: electronic structure, dielectrics, defects, traps, oxygen vacancy, resistive memory, density functional theory.

DOI: 10.61011/PSS.2025.01.60590.258

1. Introduction

Silicon oxynitride (SiO_xN_y) is one of the key materials for use as passive and active layers of elements of modern silicon microelectronics [1]. There are many studies indicating the prospects of SiO_xN_y for use as an active layer of resistive memory elements (ReRAM) [2–5]. This memory is based on a reversible change in the resistance of the dielectric layer of the metal structure−dielectric−metal due to electrochemical reactions under the influence of a current pulse in the local region of the dielectric forming a conductive filament [6]. It is proposed to use SiO_xN_y films enriched with silicon to reduce the voltage of the first dielectric switching to a low-resistance state (so-called forming) [5]. By analogy with silicon oxide and nitride, it can be expected that Si−Si bonds are the most likely intrinsic defects responsible for resistive switching of SiO_xN_y, i. e. oxygen or nitrogen vacancies [6,7]. However, Si−Si bond is a deep trap for SiO_2 and Si_3N_4 with an ionization energy of more than 1 eV [8,9], whereas charges transport in memristors based on SiO_xN_y in high-resistance state is carried our with the participation of shallow traps with an energy of the order of 10−100 meV [10]. The nature of shallow traps in silicon-enriched SiO_xN_y is currently unknown.

Thus, the study of the electronic structure of silicon-enriched SiO_xN_y, in particular, the electronic structure of intrinsic defects in SiO_xN_y, is an urgent task for understanding the physics of resistive switching of memristors to based on SiO_xN_y. An effective method for studying the electronic structure of defects in solids is ab initio modeling within the density functional theory (DFT). Existing theoretical studies are mainly limited to the study of SiO_xN_y without silicon enrichment, the atomic structure of which includes only Si−O and Si−N bonds [11–14]. The structure of silicon-enriched SiO_xN_y is significantly more complex: it is described by the Random Bonding (RB) model and contains 15 varieties of tetrahedra $Si-O(\nu)N(\mu)Si(4-\nu-\mu)$, (where $\mu+\nu=0$, 1, 2, 3, 4) in a certain proportion [4,15]. Previously, electronic structure of silicon-enriched SiO_xN_y was modeled only for a structural model far from RB [5]. Intrinsic defects in such a structure were not modeled.

The aim of this study is to theoretically study the atomic and electronic structure of SiO_xN_y of variable composition enriched in silicon in a wide range of coefficients x and y, as well as to determine the ability of defects of Si−Si bond type in SiO_xN_y to act as shallow traps in memristors based on SiO_xN_y.

2. Methods

The simulation were conducted within the DFT in a periodic cell model, a pseudopotentials approximation with a plane-wave basis in the software package Quantum ESPRESSO [16]. A series of model crystal structures of silicon-enriched SiO_xN_y width $y=0$, 0.25 and 0.5, $x=0.25$, 0.5, 0.75, 1.0, 1.25 and 1.5 were obtained as follows:

1. A 48-atom cell SiO_2 was created in β-phase of the cristabolite. This phase was chosen as the closest in physical properties to the amorphous SiO_2 [17];

2. Supercells of „SiO_x“ ($x < 2$) were created by sequentially removing a different number of pairs of oxygen atoms, considering either all or about 5 000 possible spatial configurations of the relative position of oxygen vacancies;

3. After calculations of full structural relaxation, those with the closest order to the RB model were selected from the created SiO_x structures, i. e. the proportion of tetrahedra $Si{-}O(\nu)Si(4{-}\nu)$, where $\nu = 0, 1, 2, 3, 4$, is determined by statistics:

$$W_\nu(x) = \frac{4!}{\nu!(1-\nu)!}\left(\frac{x}{2}\right)^\nu\left(1-\frac{x}{2}\right)^{4-\nu}; \qquad (1)$$

4. One structure was selected from the obtained set of potential SiO_x structures for each value of x based on the principles the supercell total energy minimum and the monotony of the dependence of the bandgap as a function of the coefficient x;

5. 4 or 8 O atoms were replaced with N in the established structures of SiO_x to obtain the compositions of $SiO_xN_{0.25}$ and $SiO_xN_{0.5}$, respectively. Either all possible substitution options were sorted out, or the order of 10^3 substitution atom locations in supercells were randomly selected;

6. Calculations of the full structural relaxation of all created supercells were performed and structures were selected for which the statistics of tetrahedra $Si{-}O(\nu)N(\mu)Si(4{-}\nu{-}\mu)$, where $(\nu+\mu) \le 4$, is the most close to the RB model:

$$W_\nu(x,y) = \frac{4!}{\nu!\mu!(1-\nu-\mu)!}\left(\frac{x}{2}\right)^\nu\left(\frac{3y}{4}\right)^\mu \times\left(1-\frac{x}{2}-\frac{3y}{4}\right)^{4-\nu-\mu}; \qquad (2)$$

7. One structure for each value of x was chosen from the set of structures of $SiO_xN_{0.25}$ and $SiO_xN_{0.5}$ found in this way according to the principle of minimum total energy of a supercell as well as the monotony of the dependence of the bandgap value as a function of the coefficient x.

Structural relaxation calculations were performed using the local exchange-correlation functional PBEsol, and the total density spectra of electronic states (TDOS) — with hybrid HSE06 functional. Calculations with the HSE06 functional were performed using optimized norm-preserving Vanderbilt pseudopotentials and the cut-off energy of the plane-wave basis 952 eV. The calculation method reproduces the bandgap value $E_g = 8.0$ eV for SiO_2 [18].

The electronic structure of intrinsic defects in SiO_xN_y was calculated by using supercells with a size of 88 to 128 atoms obtained by two or three-fold translation of the established structures of SiO_xN_y. Si−Si bonds formed either by creating an O vacancy or an N vacancy with the addition of a hydrogen atom were considered as defects capable of acting as traps for charge carriers. Each defect was modeled in all possible unequal positions of the supercells. The electronic structure was calculated for three charge states of the system (with full charge $q = 0, -1, +1$) in the framework of a spin-polarized DFT. The trap energies were estimated as an energy gain in capturing an electron from the conduction band bottom ΔE_e or a hole from the valence band topΔE_h for a defect according to the formulas proposed in Ref. [19]:

$$\Delta E_e = (E^{-1}_{\text{init}} + E^{+1}_{\text{def}}) - (E^0_{\text{init}} + E^0_{\text{def}}), \qquad (3)$$

$$\Delta E_h = (E^{+1}_{\text{init}} + E^{-1}_{\text{def}}) - (E^0_{\text{init}} + E^0_{\text{def}}). \qquad (4)$$

Here, the superscripts indicate the full charge of the supercell; E_{init} and E_{def} — the full energy of the initial and defective supercells, respectively.

3. Results

Figure 1 shows calculated TDOS spectra for model structures of SiO_xN_y of various compositions created using the above method, aligned along the edge of the lower (O 2s) valence subband, which for β-SiO_2 is located 17.9 eV below the valence band top E_v. The align along the edge of O 2s of the peak is attributable to the fact that the deep levels are least sensitive to the atomic environment. The data obtained demonstrate a shift of the edges of the valence band and the conduction band (E_c) to the band gap. The shifts of E_v and E_c are not symmetrical: E_c shifts stronger. The top of SiO_xN_y valence band is formed mainly by Si 3p atomic orbitals corresponding to the orbitals

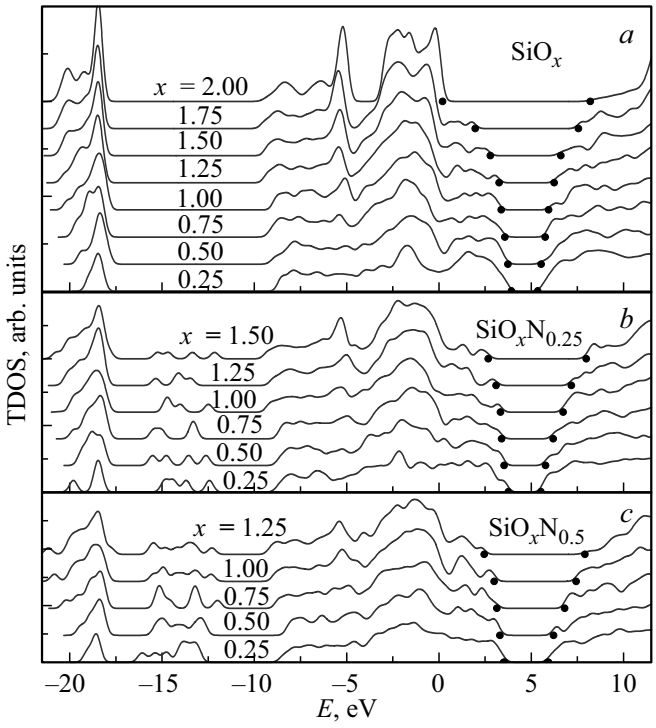

Figure 1. Spectra of total density spectra of electronic states of SiO_xN_y for three compositions: $y = 0$ (a), 0.25 (b) and 0.5 (c). Zero energy corresponds to the position of the valence band top E_v β-SiO_2; the spectra aligned along the position of the peak O 2s level at 17.9 eV below E_v and smoothed by the Gaussian function with $\sigma = 0.2$ eV.

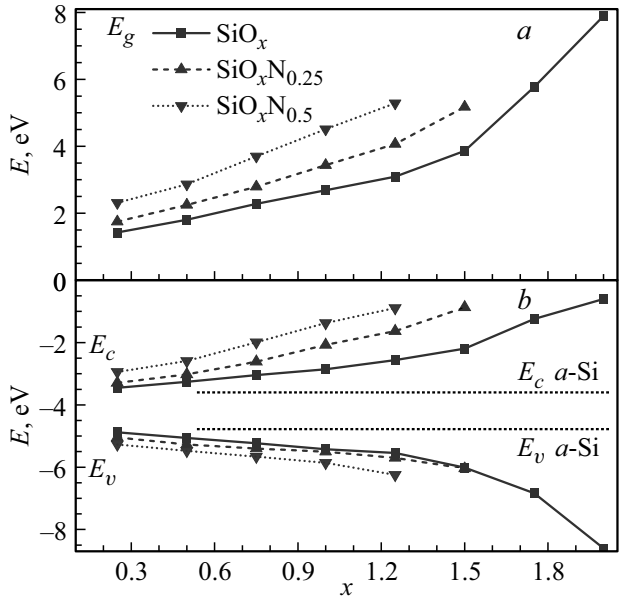

Figure 2. Theoretical dependences of the bandgap value E_g (a), as well as the positions E_v and E_c relative to the vacuum level (b) depending on the coefficient value x for SiO_xN_y with $y = 0$, 0.25 and 0.5.

of σ-Si−Si bonds. The shift of E_v towards lower bond energies due to a decrease of the oxygen content in SiO_xN_y is explained by the fact that this reduces the energies of binding σ-orbitals of Si−Si bonds as their concentration increases. The electron density near the bottom of the conduction band consists mainly of Si $3p$-orbitals with an admixture of Si $3s$. The shift of E_c into the band gap can be explained by a decrease of the energy of the anti-binding σ^*-orbitals of Si−Si bonds. Qualitatively similar TDOS spectra of SiO_xN_y are close to those previously published using significantly simpler structural models of SiO_xN_y [5], however, there are a number of quantitative differences.

According to expectations, a monotonous increase of the value of E_g is observed with an increase of the coefficient x in case of a fixed content of N (value y) in SiO_xN_y (Figure 2, a). Moreover, the rate of this growth also increases with an increase in the content of N. The value of E_g SiO_xN_y increases with the increase of coefficient y in case of a fixed O content (value x). It is important to note that the dependences $E_g(x)$ obtained in this study for $y = 0$ and 0.5 are lower than the corresponding curves for SiO_x (on average by 0.3 eV) [20] and $SiO_xN_{0.5}$ (0.7 eV on average) [5], calculated for simpler model structures with a near-range order far from the RB model. At the same time, the calculated dependence $E_g(x)$ for SiO_x RB agrees well with the theoretical curve $E_g(x)$ obtained earlier using the strong coupling method with the generalized Bethe [21] lattice model, as well as the experimental curve [20]. These data indicate the correctness of the structural model SiO_xN_y used in this work and the calculation method.

The data presented in Figure 1, including the position of E_v known from the literature relative to the vacuum level for SiO_2 [22], allows plotting an energy diagram of SiO_xN_y for various compositions (Figure 2, b). The levels E_v and E_c for Si can be superimposed on this diagram, knowing the values of electron affinity (5.2 eV) and E_g (1.6 eV) for a-Si [23]. The energy diagrams obtained in this way for silicon-enriched SiO_xN_y allow estimating the energy values of potential barriers for electrons (Φ_e) and holes (Φ_h) at the boundary of a-Si/SiO_xN_y for various compositions. As can be seen, there is a monotonous and almost linear increase of the values of Φ_e and Φ_h with an increase of coefficient x. Φ_e is greater than Φ_h for any value of coefficient x, which is also true for the boundaries Si/SiO_2 [23] and Si/Si_3N_4 [9], and this difference increases with an increase of the content of N in the material. Thus, the calculated dependences $E_g(x)$ and energy diagrams allow estimating the values of E_g, Φ_e and Φ_h by known coefficients x and y for real oxynitride films.

The localization energy values of the electron ΔE_e and holes ΔE_h on the Si−Si bond formed by creating oxygen vacancies, as well as nitrogen vacancies with the addition of hydrogen in SiO_xN_y supercells of various compositions (values x and y). Since the values of $\Delta E_e/\Delta E_h$ correspond to the electron/hole transition energies from the defect level to the levels corresponding to E_c/E_v, it is convenient to represent the calculated values of $\Delta E_e/\Delta E_h$ as levels on the energy diagrams of SiO_xN_y (see Figure 2), the position of which corresponds to $[E_c - \Delta E_e]/[E_v + \Delta E_h]$ (Figure 3). Due to the spread of values of $\Delta E_e/\Delta E_h$ depending on the modeled defect position in the supercell, as well as due to the presence of a systematic error in the method of calculation of $\Delta E_e/\Delta E_h$, which, according to our estimates, is 0.1−0.2 eV, Figure 3 shows the averaged position of defect levels in the energy band of 0.3 eV. Despite the relatively large absolute error of determination of the defect levels position in the band gap, the relative error of the method is small, which allows drawing fairly reliable conclusions based on the results, that listed below:

1. The positive calculated values of ΔE_e and ΔE_h for the modeled defects in SiO_xN_y of the studied compositions indicate that the Si−Si bonds act as a trap as for an electron, and for a hole. That is, by analogy with the stoichiometric SiO_2 [8] and Si_3N_4 [9], the Si−Si bonds in SiO_xN_y are amphoteric traps and can participate in charge transport;

2. It was found that the values of ΔE_e and ΔE_h monotonously decrease with a decrease of the value of x (content of O) with a fixed y. Similarly, a decrease of the values of ΔE_e and ΔE_h is observed with a decrease of the value of y (content of N) with a fixed x. This trend is directly correlated with the dependence $E_g(x, y)$;

3. The values of ΔE_e and ΔE_h for the Si−Si bond formed by the removal of the O atom, as well as by the removal of the N atom with the addition of H, are practically indistinguishable (within the accuracy limits of the method). Therefore, both types of studied defects make approximately the same contribution to the conductivity of SiO_xN_y;

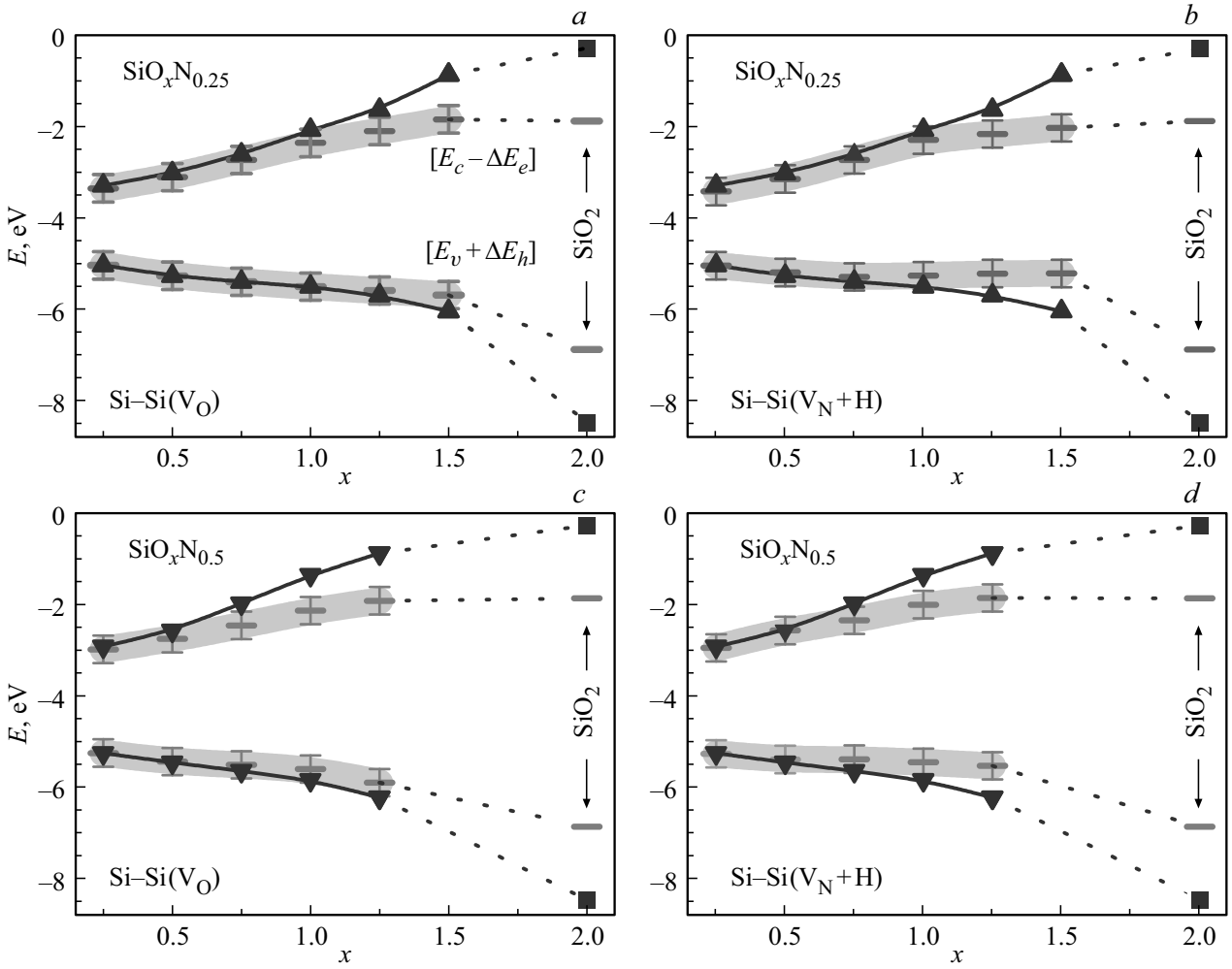

Figure 3. Position E_v and E_c for SiO_xN_y of various compositions x and $y = 0.25$ (a, b), 0.5 (c, d) relative to the vacuum level, as well as the position in the band gap of the levels of the electron (ΔE_e) and hole trap (ΔE_h) from the oxygen vacancy V_O (a, c) and from the nitrogen vacancy with hydrogen $V_N + H$ (b, d).

4. The decrease of the values of ΔE_e and ΔE_h with a decrease of both coefficients x and y is mainly attributable to the shift of E_c/E_v into the band gap, whereas the absolute position of the level of Si−Si bond in the band gap (relative to the vacuum level) slightly varies;

5. The energy values of electron localization (ionization) are only slightly higher than those for holes in SiO_xN_y, like in stoichiometric SiO_2 and Si_3N_4. Taking into account the fact that the effective masses of electrons, as a rule, are less than the effective masses of holes in solids, and also judging by the proximity of the values of Φ_e and Φ_h for different values of the coefficient x, it is possible to judge about similar contributions of the electron and hole charge transport in the conductivity of SiO_xN_y;

6. The absolute position of the defective levels (relative to the vacuum level) for electrons is above E_c(a-Si) and below E_v(a-Si) for holes for any value of x and y SiO_xN_y according to the constructed energy diagrams (Figures 2 and Figure 3);

7. The constructed energy diagrams for SiO_xN_y (Figure 3) allow making rough estimates of the trap energy values for experimentally studied SiO_xN_y films based on the preset values of the coefficients x and y;

8. The defect trap energy $\Delta E_e/\Delta E_h$ is less than 0.1 eV with sufficiently strong enrichment of SiO_xN_y with silicon (at $x < 1$ for $y = 0.25$ and $x < 0.7$ for $y = 0.5$). This proves that Si−Si bonds are defects capable of creating shallow traps with energy of the order of 10−100 meV in the high-resistance state of SiO_xN_y-based memristors. This also indicates that the conductive filament in such memristors is a highly silicon-rich dielectric region. Moreover, the degree of silicon enrichment (oxygen depletion) is higher for memristors based on SiO_xN_y with a high nitrogen content.

4. Conclusion

Structures of silicon-enriched SiO_xN_y have been created based on ab initio calculations in a wide range of

compositions, the short-range order of which corresponds to the RB model and energy diagrams of SiO_xN_y were constructed depending on the material composition. These diagrams allow estimating the bandgap values E_g and the potential barriers energy for electrons Φ_e and holes Φ_h at the boundary of a-Si/SiO_xN_y according to the known coefficients x and y for real oxynitride films. It is shown that E_g, Φ_e and Φ_h monotonously decrease with the decrease of coefficients x and y due to the shifting of the edges of the valence band E_v and conduction band E_c into the band gap of the dielectric. Moreover, E_c shifts more strongly than E_v. The electronic structure of oxygen vacancies forming Si−Si bond, as well as nitrogen vacancies with the addition of hydrogen, as the most likely defects responsible for charge transport and resistive switching of SiO_xN_y-based memristors was calculated. It has been established that these defects in SiO_xN_y can act as traps for both electrons and holes, and the depth of this trap monotonously decreases with the decrease of values of coefficients x and y mainly due to the shift of E_c/E_v into the band gap. A conclusion is made about the similarity of contributions of electron and hole charge transport to the conductivity of SiO_xN_y, i.e., about the bipolar conductivity of SiO_xN_y. It has been established that Si−Si bonds with sufficiently strong enrichment of SiO_xN_y with silicon are the defects capable of producing shallow traps in the high-resistance and low-resistance states of SiO_xN_y-based memristors.

Funding

The study was conducted within the framework of the state assignment of the Ministry of Science and Higher Education of the Russian Federation (topic No. FWGW-2025-0023). Ab initio simulating was carried out using the resources of the NSU Computing Center.

Conflict of interest

The authors declare that they have no conflict of interest.

References

[1] Y. Shi, L. He, F. Guang, L. Li, Z. Xin, R. Liu. Micromachines **10**, *8*, 552 (2019).
[2] N.C. Das, S.-I. Oh, J.R. Rani, S.-M. Hong, J.-H. Jang. Appl. Sci. **10**, *10*, 3506 (2020).
[3] K. Leng, X. Zhu, Z. Ma, X. Yu, J. Xu, L. Xu, W. Li, K. Chen. Nanomaterials **12**, *3*, 311 (2022).
[4] Y.N. Novikov, G.N. Kamaev, I.P. Prosvirin, V.A. Gritsenko. Appl. Phys. Lett. **122**, 232903 (2023).
[5] T.V. Perevalov, V.A. Volodin, G.N. Kamaev, A.A. Gismatulin, S.G. Cherkova, I.P. Prosvirin, K.N. Astankova, V.A. Gritsenko. J. Non-Cryst. Solids, **598**, 121925 (2022). https://doi.org/10.1016/j.jnoncrysol.2022.121925
[6] A. Mehonic, A.L. Shluger, D. Gao, I. Valov, E. Miranda, D. Ielmini, A. Bricalli, E. Ambrosi, C. Li, J.J. Yang, Q. Xia, A.J. Kenyon. Adv. Mater. **30**, *43*, 1801187 (2018).
[7] T.J. Yen, A. Chin, V. Gritsenko, Nanomaterials, **11**, *6*, 1401 (2021).
[8] D.R. Islamov, V.A. Gritsenko, T.V. Perevalov, O.M. Orlov, G.Ya. Krasnikov. Appl. Phys. Lett. **109**, 052901 (2016).
[9] V.A. Gritsenko, T.V. Perevalov, O.M. Orlov, G.Ya. Krasnikov. Appl. Phys. Lett. **109**, 062904 (2016).
[10] A.A. Gismatulin, G.N. Kamaev, V.A. Volodin, V.A. Gritsenko. Electronics **12**, 598 (2023).
[11] A.N. Sorokin, A.A. Karpushin, V.A. Gritsenko, H. Wong. J. Appl. Phys. **105**, 073706 (2009).
[12] Z.-L. Lv, H.-L. Cui, H. Wang, X.-H. Li, G.-F. Ji. Ceram. Int. **43**, 10006 (2017).
[13] A. Martinez-Limia, P. Plänitz, C. Radehaus. Phys. Rev. B **73**, 165213 (2006).
[14] Z.-G. Duan, Z.-Y. Zhao, P.-Z. Yang. RSC Adv. **4**, 36485 (2014).
[15] P. Cova, S. Poulin, O. Grenier, R.A. Masut. J. Appl. Phys. **97**, 073518 (2005).
[16] P. Giannozzi, O. Andreussi, T. Brumme, O. Bunau, M.B. Nardelli, M. Calandra, R. Car, C. Cavazzoni, D. Ceresoli, M. Cococcioni, N. Colonna, I. Carnimeo, A. Dal Corso, S. de Gironcoli, P. Delugas, R.A. DiStasio, A. Ferretti, A. Floris, G. Fratesi, G. Fugallo, R. Gebauer, U. Gerstmann, F. Giustino, T. Gorni, J. Jia, M. Kawamura, H.Y. Ko, A. Kokalj, E. Kucukbenli, M. Lazzeri, M. Marsili, N. Marzari, F. Mauri, N.L. Nguyen, H.V. Nguyen, A. Otero-de-la-Roza, L. Paulatto, S. Ponce, D. Rocca, R. Sabatini, B. Santra, M. Schlipf, A.P. Seitsonen, A. Smogunov, I. Timrov, T. Thonhauser, P. Umari, N. Vast, X. Wu, S. Baroni. J. Phys-Condens. Mat. **29**, 465901 (2017).
[17] D.A. Keen, M.T. Dove. J. Phys.: Condensed Matter, **11**, *47*, 9263 (1999).
[18] R. Williams. Phys. Rev. **140**, A569 (1965).
[19] A.S. Foster, F. Lopez Gejo, A.L. Shluger, R.M. Nieminen. Phys. Rev. B **65**, 174117 (2002).
[20] T.V. Perevalov, V.A. Volodin, Yu.N. Novikov, G.N. Kamaev, V.A. Gritsenko, I.P. Prosvirin. FTT **61**, *12*, 2528 (2019). (in Russian).
[21] A.A. Karpushin, V.A. Gritsenko. Pis'ma v ZhETF **108**, 114 (2018). (in Russian).
[22] D.T. Pierce, W.E. Spicer. Phys. Rev. B **5**, 3017 (1972).
[23] N. Fujimura, A. Ohta, K. Makihara, S. Miyazaki. Jap. J. Appl. Phys. **55**, 08PC06 (2016).

Translated by A.Akhtyamov